

GPS-Synchronized Dynamic Data Acquisition: Technology Assessment and Applications

A. P. Sakis Meliopoulos and George J. Cokkinides
School of Electrical and Computer Engineering
Georgia Institute of Technology
Atlanta, GA 30332
Sakis.m@gatech.edu

Abstract

GPS-synchronized equipment (PMUs) is in general higher precision equipment as compared to typical SCADA systems. Conceptually, PMU data are time tagged with accuracy of better than 1 microsecond and magnitude accuracy that is better than 0.1%. This potential performance is not achieved in an actual field installation due to errors from instrumentation channels and system imbalances. Presently, PMU data precision from substation installed devices is practically unknown. On the other hand, specific applications of PMU data require specific accuracy of data. Applications vary from simple system monitoring to wide area protection and control to voltage instability prediction. Each application may have different accuracy requirements. For example for simple system monitoring in steady state highly accurate data may not be critical while for transient instability prediction high precision may be critical. For addressing data precision requirements for a variety of applications, it is necessary to quantify the accuracy of the collected PMU data. We discuss data precision requirements for a variety of applications and we propose a methodology for characterizing data errors. In particular, we propose a new approach for improving data accuracy via estimation methods. The proposed methodology quantifies the expected error of the filtered data. Examples are provided that define the instrumentation requirements for specific applications. This approach enables a number of advanced applications, such as distributed state estimation, transient stability monitoring and wide area dynamic monitoring of the power system.

Keywords: GPS-synchronized equipment, Data Accuracy, State Estimation

Glossary

GPS: Global Positioning System

PMU: Phasor Measurement Unit

CT: Current Transformer

VT: Voltage Transformer

CCVT : Capacitor Coupled Voltage Transformer

1. Introduction

GPS-synchronized equipment (PMUs) is in general higher precision equipment as compared to typical SCADA systems. Conceptually, PMUs provide measurements that are time tagged with precision better than 1 microsecond and magnitude accuracy that is better than 0.1%. This potential performance is not achieved in an actual field installation because of two reasons: (a) different vendors use different design approaches that result in variable performance among vendors, for example use of multiplexing among channels or variable time latencies among manufacturers result in timing errors much greater than one microsecond, and (b) GPS-synchronized equipment receives inputs from instrument transformers, control cables, attenuators, etc. which introduce magnitude and phase errors that are much greater than the precision of PMUs. For example, many utilities may use CCVTs for instrument transformers. We refer to the errors introduced by instrument transformers, control cables, attenuators, etc. as the instrumentation channel error. Appendix A presents quantitative results of errors introduced by instrumentation channels. The end result is that “raw” phasor data from different vendors cannot be used as highly accurate data.

GPS-synchronized data offer the possibility of dramatically improved applications, such as real time monitoring of the system, improved state estimation, direct state measurement, precise disturbance monitoring, transient instability prediction, wide area protection and

control, voltage instability prediction and many others. For proper functioning of each one of these applications, a certain precision of the data is required. Present research activities focus on defining data precision requirements for each possible application of GPS-synchronized data under the EIPP performance requirements tasks. Once the necessary data precision requirements for an application have been defined, it is now necessary to characterize the actual precision of the data.

Application	Required Data Accuracy
Steady State Monitoring	Low
Disturbance Monitoring	Moderate
State Measurement	High
State Estimation	High
Wide Area Protection	Moderate
Transient Instability Monitoring	High

Conceptually, the overall precision issue can be resolved with sophisticated calibration methods. This approach is quite expensive and faces difficult technical problems. It is extremely difficult to calibrate instrument transformers and the overall instrumentation channel in the field. Laboratory calibration of instrument transformers is possible but a very expensive proposition if all instrument transformers need to be calibrated. In the early 90's the authors directed a research project in which we developed calibration procedures for selected NYPA's high voltage instrument transformers [9]. From the practical point of view, this approach is an economic impossibility. An alternative approach is to utilize appropriate filtering techniques for the purpose of correcting the magnitude and phase errors, assuming that the characteristics of the various GPS-synchronized equipment are known and the instrumentation feeding this equipment is also known.

We propose a viable and practical approach to correct for errors from instrumentation, system imbalances and data acquisition systems. The approach is based on an estimation process at the substation level for correcting these errors. Specifically, we propose a methodology that performs as a "super-calibrator". This method and computational procedure may reside at the substation, and it can operate on the streaming data. The process is fast and therefore it can be applied on real time data on a continuous basis introducing only minor time latencies. Specifically, our analysis has determined that the filtering can be performed within few milliseconds on a high end personal computer for a typical substation that may have several hundreds of data to be filtered and assuming that the filtering algorithm has been optimized. This efficiency can support streaming data flow of 30 samples per second with only few milliseconds delay on the streaming data,

since for this data rate, there is at least 20 milliseconds of free time between each data packet. The procedure does maintain the data format including the time tags of the data. The proposed methodology is based on a statistical estimation methodology that requires (a) the characteristics of GPS-synchronized equipment (PMUs) and (b) a detailed model of the substation including the model of the instrumentation. Subsequent paragraphs present the models of the GPS-synchronized equipment as well as the substation model with the instrumentation channels.

2. Method Description

The methodology is based on a detailed, integrated model of the power system, instrumentation channel and data acquisition system. The power system model is a detailed three-phase, breaker oriented model and includes the substation and the interconnected transmission lines. The instrumentation channel model includes instrument transformers, control cables, attenuators, burdens, and A/D converters. The modeling approach is physically based, i.e. each model is represented with the exact construction geometry and the electrical parameters are extracted with appropriate computational procedures. As the data stream, each set of data at a specific time tag is processed via a general state estimation process that "fits" the data to the integrated model. The procedure provides the best estimate of the data as well as performance metrics of the estimation process. The most important metric is the expected value of the error of the estimates. The best estimate of the data is used to regenerate the streaming data flow (this data is now filtered). The overall approach is illustrated in Figure 1.

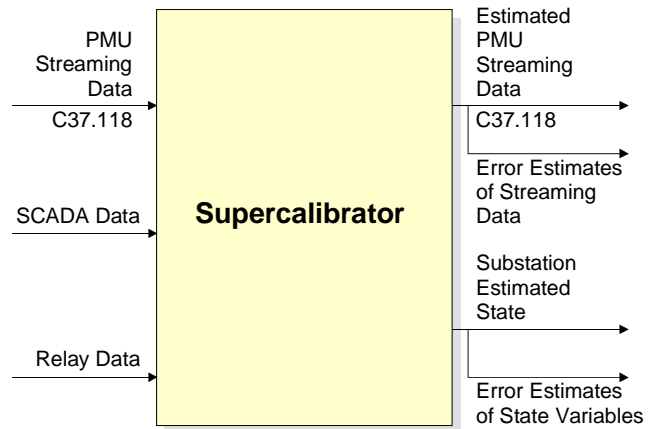


Figure 1. Inputs and Outputs of the Super-Calibrator

It is important to note that the proposed methodology (which we have named the super-calibrator) is also a tool for remote calibration. Since these equipment are digital and since the super-calibrator will determine what the

“reading” of each device should be, a calibration factor can be inserted into each channel of the GPS-synchronized equipment. This very simple method is also very effective.

3. Substation State Estimation

Instrumentation and other measurement data errors are filtered with state estimation methods. We describe two approaches for this process: (a) a static state estimation method and (b) a dynamic state estimation method. To introduce the method, consider the single line diagram of the substation of Figure 2. The state of the system is defined as the minimum number of independent variables that completely define the state of the system. For the substation of Figure 1 the state of the system consists of: (a) the phasor voltages of phase A, B and C of buses BW-AUTO-S, BW-AUTO-H, BW-AUTO-T and BAX-W-GU2 (a total of twelve complex numbers), and (b) the phasor currents of phase A, B and C for currents at the circuits LINE1, LINE2, and LINE3 (a total of nine complex numbers). In summary, the state of the substation of Figure 2 is defined in terms of 21 complex variables.

The number of measurements for this system from GPS-synchronized equipment, relays and standard SCADA system is quite large. Typically, the direct voltage measurements alone will have a redundancy of two to three, i.e. two to three times the number of voltage states. The available current measurements will generate a much larger redundancy considering that there will be CTs at each breaker, transformer, reactors, etc. For the system of Figure 2, and with a typical instrumentation, there will be more than 120 measurement data. This represents a redundancy level of 570%.

The state of the system is defined as the phasors of the phase voltages at each bus and selected electric current on outgoing transmission lines. A bus k will have three to five nodes, phases A, B and C, possibly a neutral and possibly a ground node. Under normal conditions the voltage at the neutral or ground will be very small and it will be assumed to be zero for this application. The state of the system at this bus is the node voltage phasors. We will use the following symbols.

$$\begin{aligned}\tilde{V}_{k,A} &= \tilde{V}_{k,A} = V_{k,A,r} + jV_{k,A,i} \\ \tilde{V}_{k,B} &= \tilde{V}_{k,B} = V_{k,B,r} + jV_{k,B,i} \\ \tilde{V}_{k,C} &= \tilde{V}_{k,C} = V_{k,C,r} + jV_{k,C,i}\end{aligned}$$

Similarly the “state” currents in a line (k,m) will be defined with:

$$\begin{aligned}\tilde{I}_{km,A} &= I_{km,A,r} + jI_{km,A,i} \\ \tilde{I}_{km,B} &= I_{km,B,r} + jI_{km,B,i} \\ \tilde{I}_{km,C} &= I_{km,C,r} + jI_{km,C,i}\end{aligned}$$

The state of the system is defined by the vector x which contains all above real variables.

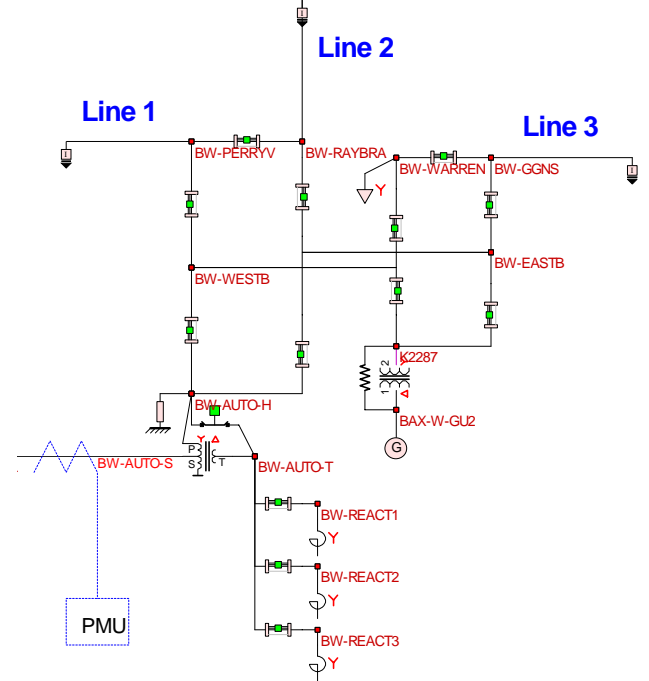


Figure 2. Breaker-Oriented Three-Phase Substation Model

The measurements can be GPS-synchronized measurements, relay data or usual SCADA data. A typical list of measurement data is given in Table 1. The measurements are assumed to have an error that is statistically described with the meter accuracy.

Table 1. List of Measurements

Phasor Measurements	Non-Synchronized Measurements
Description	Description
Voltage Phasor, \tilde{V}	Voltage Magnitude, V
Current Phasor, \tilde{I}	Real Power Flow, P_f
Current Inj. Phasor, \tilde{I}_{inj}	Reactive Power Flow, Q_f
	Real Power Injection, P_{inj}
	Reactive Power Inj., Q_{inj}

Each measurement is related to the state of the system via a function. An innovation presented here is the addition of the instrumentation channel model in the overall model of each measurement. Specifically, consider measurement j , represented with the variable y_j . This measurement can be a GPS-synchronized measurement (phasor) or a non-synchronized measurement (scalar). Consider the instrumentation channel model and the transfer function of the instrumentation channel for this measurement defined with the function $g_j(f)$, f : frequency. Then the measurement on the power system side, z_j , is:

$$z_j = \frac{y_j}{g_j(f = 60\text{Hz})}$$

Each measurement, z_j , can be expressed as a function of the substation state. We provide here examples of measurements and the mathematical expression that relates the measurement to the state.

Phasor measurement of voltage: Consider the phasor measurement of the phase A voltage of BUS161. The model for this measurement is:

$$z_{r1} + jz_{i1} = G_1 e^{j\alpha_1} (\tilde{V}_{1,a} - \tilde{V}_{1,n})$$

Phasor measurement of state current: Consider the phasor measurement of the phase A current of line L1. The model for this measurement is:

$$z_{r2} + jz_{i2} = G_2 e^{j\alpha_2} (\tilde{I}_{L1,a})$$

Given a set of measurements, the state of the system is computed via the well known least square approach. Specifically, let z_i be a measurement and $h_i(x)$ be the function that relates the quantity of the measurement to the state of the system. The state is computed from the solution of the following optimization problem.

$$\text{Min } J = \sum_i \left(\frac{z_i - h_i(x)}{\sigma_i} \right)^2$$

where σ_i is the meter accuracy.

Solution methods for above problem are well known. In subsequent paragraphs, the models of the measurements and the details of the hybrid state estimator are described.

4. Description of Measurement Model

This section presents the overall measurement model. It consists of two parts. Part 1 is the model of the instrumentation channel. Part 2 is the model of the observed quantity as a function of the substation model. Both models are briefly described below.

Instrumentation Channel Model: PMUs, SCADA, Relaying, metering and disturbance recording use a system of instrument transformers to scale the power system voltages and currents into instrumentation level voltages and currents. Standard instrumentation level voltages and currents are 67V or 115V and 5A respectively. These standards were established many years ago to accommodate the electromechanical relays. Today, the instrument transformers are still in use but because modern relays, metering and disturbance recording operates at much lower voltages, it is necessary to apply another transformation from the previously defined standard voltages and currents to another set of standard voltages of 10V or 2V. This means that the modern instrumentation channel consists of typically two transformations and additional wiring and possibly burdens. Figure 3 illustrates typical instrumentation channels, a voltage channel and a current channel.

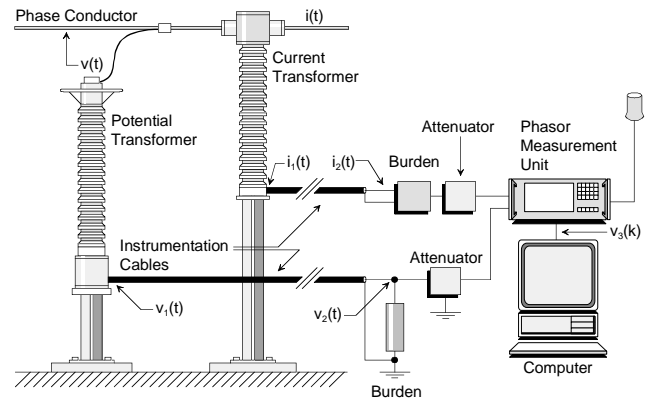


Figure 3. Typical Instrumentation Channel for PMU/Relay/IED Data Collection

Note that each component of the instrumentation channel will introduce an error. Of importance is the net error introduced by all the components of the instrumentation channel. The overall error can be defined as follows. Let the voltage or current at the power system be:

$$v_a(t), \quad i_a(t)$$

An ideal instrumentation channel will generate a waveform at the output of the channel that will be an exact replica of the waveform at the power system. If the

nominal transformation ratio is k_v and k_i for the voltage and current instrumentation channels respectively, then the output of the ideal channels will be:

$$v_{ideal}(t) = k_v v_a(t), \quad i_{ideal}(t) = k_i i_a(t)$$

The error is defined as follows:

$$v_{error}(t) = v_{out}(t) - v_{ideal}(t), \quad i_{error}(t) = i_{out}(t) - i_{ideal}(t)$$

where the subscript “out” refers to the actual output of the instrumentation channel. The error waveform can be analyzed to provide the rms value of the error, the phase error, etc. The overall instrumentation channel error can be characterized with the gain function of the entire channel defined with (for voltage and current measurement respectively):

$$g_{j,v}(f) = \frac{\tilde{V}_{out}(f)}{\tilde{V}_{in}(f)} \quad \text{and} \quad g_{j,i}(f) = \frac{\tilde{I}_{out}(f)}{\tilde{I}_{in}(f)}$$

The instrumentation error can be computed by appropriate models of the entire instrumentation channel. It is important to note that some components may be subject to saturation (CTs and PTs) while other components may include resonant circuits with difficult to model behavior (CCVTs), see reference [2,6]. The detailed models of the instrumentation channels is discussed in reference [2] and it is not repeated here. As an example, Figures 4 and 5 illustrate the computer generated instrumentation channel models for a current and voltage measurement respectively.

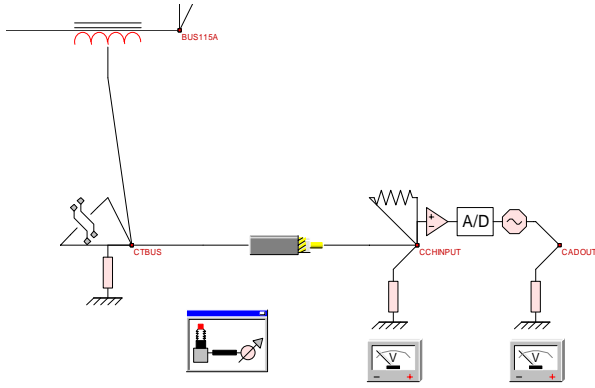


Figure 4. Computer Model of an Instrumentation Channel, CT Based

Measurement Data Model: The available data in a power system can be classified into (a) phasor measurements (GPS synchronized measurements) and (b) non-synchronized measurements. A typical list of measurements has been given in Table 1. As it has been

mentioned, the measurements are related to the state of the system via the “model” equations. The state of the system has been defined in the previous section. The model equations, i.e. the equations that relate the substation state to the measurement are given below.

$$z_{V,k,A} = g_{V,k,A} (60\text{Hz}) \tilde{V}_{k,A}$$

$$z_{V,k,A} = g_{V,k,A} (60\text{Hz}) \tilde{V}_{k,A}$$

$$z_{V,k,A} = g_{V,k,A} (60\text{Hz}) \tilde{V}_{k,A}$$

$$\tilde{I}_{d1,k,A} = C_{d1,k,A}^T x, \quad \text{similarly for phases B and C.}$$

$$V_{k,A} = g_{k,A} (60\text{Hz}) \sqrt{V_{k,A,r}^2 + V_{k,A,i}^2}$$

$$P_{d1,k,A} = g_{pd1,k,A} (60\text{Hz}) \text{Re} \left\{ \tilde{V}_{k,A} C_{d1,k,A}^T \begin{bmatrix} \tilde{V}_{k,A} \\ \tilde{V}_{k,B} \\ \tilde{V}_{k,C} \\ \tilde{V}_{m,A} \\ \tilde{V}_{m,B} \\ \tilde{V}_{k,C} \end{bmatrix} \right\}^*$$

$$Q_{d1,k,A} = g_{qd1,k,A} (60\text{Hz}) \text{Im} \left\{ \tilde{V}_{k,A} C_{d1,k,A}^T \begin{bmatrix} \tilde{V}_{k,A} \\ \tilde{V}_{k,B} \\ \tilde{V}_{k,C} \\ \tilde{V}_{m,A} \\ \tilde{V}_{m,B} \\ \tilde{V}_{k,C} \end{bmatrix} \right\}^*$$

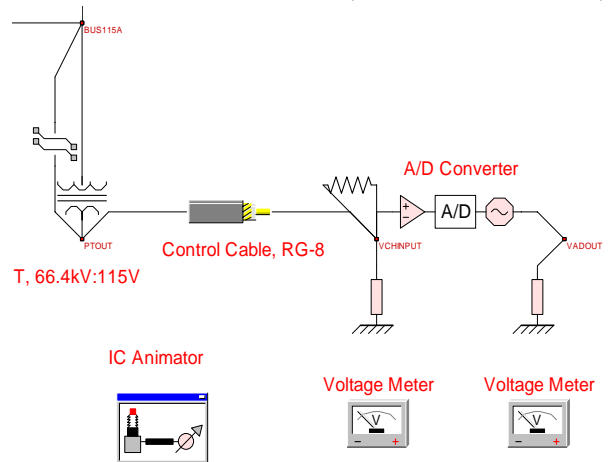


Figure 5. Computer Model of a Voltage Instrumentation Channel, PT Based

To facilitate the definition and the measurements and to devise a scheme for interfacing with the three-phase quadratized power system model, each measurement is defined with the following set:

$$S_{meas} = \{m_{type} \quad n_{device} \quad n_{bus} \quad n_{phase}\}$$

where:

m_{type} : measurement type defined as in Table 3.1

n_{device} : power device ID, plus manufacturer and IED (relay, RTU, etc.) ID

n_{bus} : bus name

n_{phase} : measurement phase, A, B or C

The above set allows complete correspondence between measurement and system state.

5. Description of the Hybrid Three-Phase State Estimator

The hybrid three-phase state estimator uses standard SCADA data and synchronized data together with a full three-phase system model to estimate the system state. The measurement data has been discussed in the previous section. The measurements are assumed to have an error that is statistically described with the meter accuracy. As an example, the measurement of a phase voltage phasor has the following mathematical model.

$$z_{V,k,A} = g_{V,k,A}(60Hz)\tilde{V}_{k,A} + \tilde{\eta}_{V,k,A}$$

where $\tilde{\eta}_{V,k,A}$ is the measurement error.

In general, the measurements will have a general form as follows:

GPS-synchronized measurements:

$$z_s = H_s x + \eta_s$$

Non-synchronized measurements

$$z_n = H_n x + \{x^T Q_i x\} + \eta_n$$

Note that the GPS-synchronized measurements are linear with respect to the substation state, while the non-synchronized measurements are quadratic with respect to the substation state.

Now, the state estimation problem is formulated as follows:

$$\text{Min } J = \sum_{v \in \text{phasor}} \frac{\tilde{\eta}_v^* \tilde{\eta}_v}{\sigma_v^2} + \sum_{v \in \text{non-syn}} \frac{\eta_v \eta_v}{\sigma_v^2}$$

It is noted that if all measurements are synchronized the state estimation problem becomes linear and the solution is obtained directly. In the presence of the non-synchronized measurements and in terms of above formulation, the problem is quadratic, consistent with the quadratized power flow. Specifically, using the quadratic formulation and the separation of the measurements into phasor and non-synchronized measurements as has been indicated earlier and repeating these equations:

$$z_s = H_s x + \eta_s$$

$$z_n = H_n x + \{x^T Q_i x\} + \eta_n$$

In above equations, the subscript s indicates phasor measurements while the subscript n indicates non-synchronized measurements. The best state estimate is given by:

Case 1: Phasor measurements only.

$$\hat{x} = (H_s^T W H_s)^{-1} H_s^T W z_s$$

Case 2: Phasor and non-synchronized measurements.

$$\hat{x}^{v+1} = \hat{x}^v + (H^T W H)^{-1} H^T W \begin{bmatrix} z_s - H_s \hat{x}^v \\ z_n - H_n \hat{x}^v - \{ \hat{x}^{v^T} Q_i \hat{x}^v \} \end{bmatrix}$$

where:

$$W = \begin{bmatrix} W_s & 0 \\ 0 & W_n \end{bmatrix}, \quad H = \begin{bmatrix} H_s \\ H_n + H_{qn} \end{bmatrix}$$

6. Implementation

The proposed methodology for correcting errors from various manufacturers is being implemented into a general state estimation method. The computer model has been named the ‘‘super-calibrator’’. Presently the methodology

operates on the data from one substation at a time. The overall approach is shown in Figure 6.

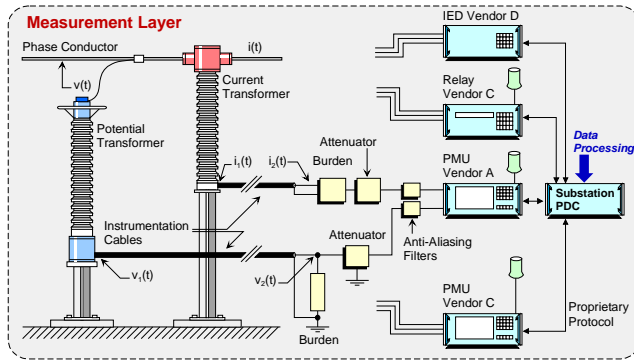


Figure 6. Conceptual Illustration of the Super-Calibrator

7. Conclusions

This paper presented a method for filtering the phasor data, relay data and SCADA data at the substation level. The innovations presented here is that the entire filtering process is confined to the substation, the instrumentation channels are explicitly represented and the substation model is a breaker-oriented three-phase model. The methodology provides the means for correcting errors from instrumentation channels, phase shifts of different PMU manufacturers and accommodates unbalanced operation and system model asymmetries.

The proposed super-calibrator provides a precise state estimator for power systems at the substation level. There are two additional major benefits: (a) it also provides the means for remote calibration. Specifically, since the system is digital, and since each measurement is analyzed in terms of raw data as well as best estimate of the measurement and best estimate of calibration error, one can trace this data. For any measurement that consistently shows a certain error and in the same direction, the raw data may be adjusted with a calibration constant. As a matter of fact, once calibration constants have been introduced for all measurements and if the super-calibrator operates with very small estimated errors, then one can simply accept the measurements without filtering. Then the filtering can be performed periodically just to make sure that nothing has changed in the system. (b) the proposed method also provides the means to minimize data communications. Specifically, the raw measurement data in a substation is enormous. On the other hand the state of a substation includes a relatively small number of variables. By estimating the substation state “on-site” it is then enough to transmit the estimated state versus the raw data. This approach minimizes the amount of data that need to be transferred. Since communications is many

times the bottleneck in a large system, obviously this approach also mitigates the communication problem.

8. Acknowledgments

The work reported in this paper has been partially supported by the NSF Grant No. 000812. This support is gratefully acknowledged.

9. References

- [1] A. P. Sakis Meliopoulos and George J. Cokkinides, “A Virtual Environment for Protective Relaying Evaluation and Testing”, *IEEE Transactions of Power Systems*, Vol. 19, No. 1, pp. 104-111, February, 2004.
- [2] A. P. Sakis Meliopoulos and G. J. Cokkinides, “Visualization and Animation of Instrumentation Channel Effects on DFR Data Accuracy”, Proceedings of the 2002 Georgia Tech Fault and Disturbance Analysis Conference, Atlanta, Georgia, April 29-30, 2002
- [3] T. K. Hamrita, B. S. Heck and A. P. Sakis Meliopoulos, ‘On-Line Correction of Errors Introduced By Instrument Transformers In Transmission-Level Power Waveform Steady-State Measurements’, *IEEE Transactions on Power Delivery*, Vol. 15, No. 4, pp 1116-1120, October 2000.
- [4] A. P. Sakis Meliopoulos and George J. Cokkinides, “Virtual Power System Laboratories: Is the Technology Ready?”, *Proceedings of the 2000 IEEE/PES Summer Meeting*, Seattle, WA, July 16-20, 2000.
- [5] A. P. Sakis Meliopoulos and George J. Cokkinides, ‘A Virtual Environment for Protective Relaying Evaluation and Testing’, *Proceedings of the 34th Annual Hawaii International Conference on System Sciences*, p. 44 (pp. 1-6), Wailea, Maui, Hawaii, January 3-6, 2001.
- [6] A. P. Sakis Meliopoulos, George J. Cokkinides, “Visualization and Animation of Protective Relays Operation From DFR Data”, *Proceedings of the 2001 Georgia Tech Fault and Disturbance Analysis Conference*, Atlanta, Georgia, April 30-May 1, 2001.
- [7] A. P. Meliopoulos and J. F. Masson, "Modeling and Analysis of URD Cable Systems," *IEEE Transactions on Power Delivery*, vol. PWRD-5, no. 2, pp. 806-815, April 1990.
- [8] G. P. Christoforidis and A. P. Sakis Meliopoulos, "Effects of Modeling on the Accuracy of Harmonic Analysis," *IEEE Transactions on Power Delivery*, vol. 5, no. 3, pp.1598-1607, July 1990.
- [9] A. P. Meliopoulos, F. Zhang, S. Zelingher, G. Stillmam, G. J. Cokkinides, L. Coffeen, R. Burnett, J. McBride, 'Transmission Level Instrument Transformers and Transient Event Recorders Characterization for Harmonic Measurements,' *IEEE Transactions on Power Delivery*, Vol 8, No. 3, pp 1507-1517, July 1993.
- [10] B. Fardanesh, S. Zelingher, A. P. Sakis Meliopoulos, G. Cokkinides and Jim Ingleson, ‘Multifunctional Synchronized Measurement Network’, *IEEE Computer Applications in Power*, Volume 11, Number 1, pp 26-30, January 1998.

[11] A. P. Sakis Meliopoulos and G. J. Cokkinides, "Phasor Data Accuracy Enhancement in a Multi-Vendor Environment", Proceedings of the 2005 Georgia Tech Fault and Disturbance Analysis Conference, Atlanta, Georgia, April 25-26, 2005

10. Biographies

A. P. Sakis Meliopoulos (M '76, SM '83, F '93) was born in Katerini, Greece, in 1949. He received the M.E. and E.E. diploma from the National Technical University of Athens, Greece, in 1972; the M.S.E.E. and Ph.D. degrees from the Georgia Institute of Technology in 1974 and 1976, respectively. In 1971, he worked for Western Electric in Atlanta, Georgia. In 1976, he joined the Faculty of Electrical Engineering, Georgia Institute of Technology, where he is presently a professor. He is active in teaching and research in the general areas of modeling, analysis, and control of power systems. He has made significant contributions to power system grounding, harmonics, and reliability assessment of power systems. He is the author of the books, *Power Systems Grounding and Transients*, Marcel Dekker, June 1988, *Lighning and Overvoltage Protection*, Section 27, Standard Handbook for Electrical Engineers, McGraw Hill, 1993, and the monograph, *Numerical Solution Methods of Algebraic Equations*, EPRI monograph series. Dr. Meliopoulos is a member of the Hellenic Society of Professional Engineering and the Sigma Xi.

George Cokkinides (M '85) was born in Athens, Greece, in 1955. He obtained the B.S., M.S., and Ph.D. degrees at the Georgia Institute of Technology in 1978, 1980, and 1985, respectively. From 1983 to 1985, he was a research engineer at the Georgia Tech Research Institute. Since 1985, he has been with the University of South Carolina where he is presently an Associate Professor of Electrical Engineering. His research interests include power system modeling and simulation, power electronics applications, power system harmonics, and measurement instrumentation. Dr. Cokkinides is a member of the IEEE/PES.

Appendix A

This Appendix provides characterization of errors resulting from instrumentation channels. The instrumentation channel may be current (CT based) or voltage (PT based or CCVT based).

A.1 CT Steady State Response

The conventional CT steady state response is very accurate. The steady state response can be extracted from

the frequency response of the device. Figure B.1 provides a typical frequency response of a CT. Note that the response is flat in the frequency range of interest. It is important to note that errors may be present due to inaccurate determination of the transformation ratio. These errors are typically small.

A.2 PT Steady State Response

Wound type PTs are in general less accurate than CTs. Again the steady state response can be obtained from the frequency response of the device. Figure B.2 provides a typical frequency response of a wound type PT. Note that the response is flat in a small frequency range around the nominal frequency. Our work has shown that the higher the transformation ratio of the PT the higher the errors will be.

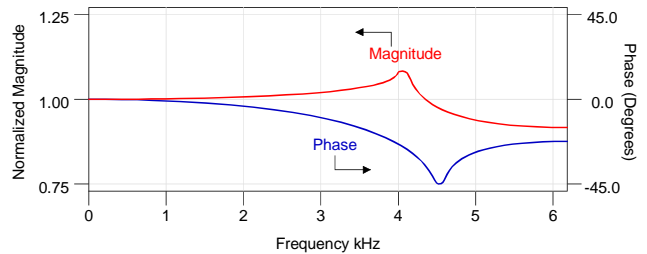


Figure A.1: Typical 600 V Metering Class CT Frequency Response

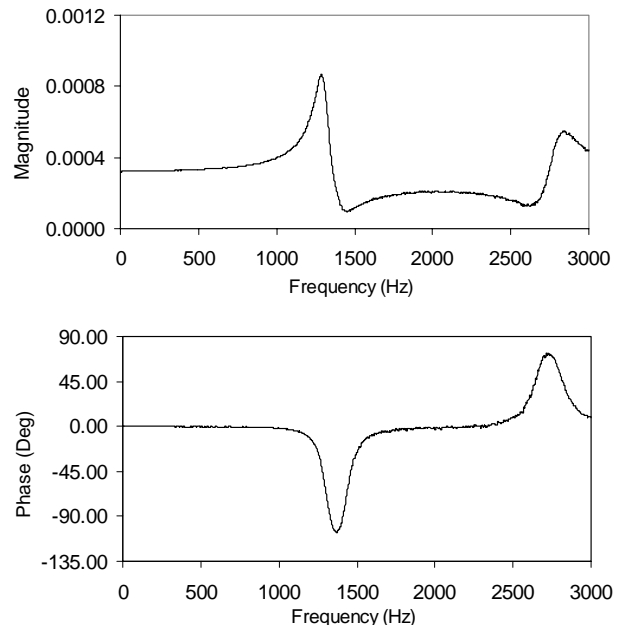


Figure A.2: 200kV/115V Potential Transformer Frequency Response

A.3 CCVT Steady State Response

By appropriate selection of the circuit components a CCVT can be designed to generate an output voltage with any desirable transformation ratio and most importantly with zero phase shift between input and output voltage waveforms. In this section we examine the possible deviations from this ideal behavior due to various causes by means of a parametric analysis, namely:

- Power Frequency Drift
- Circuit component parameter Drift
- Burden Impedance

The parametric analysis was performed using the CCVT equivalent circuit model illustrated in Figure B.3. The model parameters are given in Table B.1:

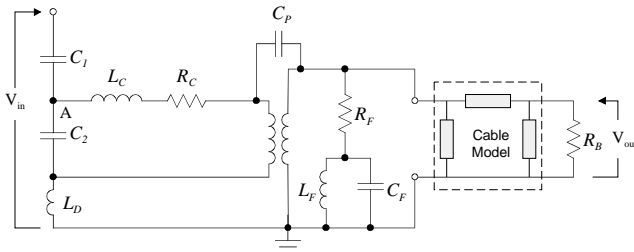


Figure A.3: CCVT Equivalent Circuit

Table A.1: CCVT Equivalent Circuit Parameters

Parameter Description	Schematic Reference	Value
CCVT Capacitance Class		Normal
Input Voltage		288 kV
Output Voltage		120 V
Upper Capacitor Size	C1	1.407 nF
Lower Capacitor Size	C2	99.9 nF
Drain Inductor	L _D	2.65 mH
Compensating Reactor Inductance	L _C	68.74 H
Compensating Reactor Resistance	R _C	3000 Ohms
Burden Resistance	R _B	200 Ohms
Ferroresonance Suppression Damping Resistor	R _F	70 Ohms
Ferroresonance Suppression Circuit Inductor	L _F	0.398 H
Ferroresonance Suppression Circuit Capacitor	C _F	17.7 uF
Cable Type		RG-8
Cable Length		100 Feet
Transformer Power Rating		300 VA
Transformer Voltage Rating		4kV/120V

Leakage Reactance		3%
Parasitic Capacitance	C _P	500 pF

Figure A.4 shows the results of a frequency scan. Note that over the frequency range of 0 to 500 Hz the response varies substantially both in magnitude and phase. Near 60 Hz (55 to 65 Hz) the response magnitude is practically constant but the phase varies at the rate of 0.25 degrees per Hz.

Table A.2 shows the results of a parametric analysis with respect to Burden resistance and instrumentation cable length. Note that the system is tuned for zero phase error for a short instrumentation cable and with a 200 Ohm Burden.

Table A.3 shows the results of a parametric analysis with respect to CCVT component parameter inaccuracies. Specifically the varied parameters were the compensating reactor inductance and the capacitive divider capacitance.

Table A.2: Phase Error (in Degrees) Versus Burden Resistance and Cable Length

Burden Resistance	Cable Length (feet)		
	10'	1000'	2000'
50 Ohms	0.077	-0.155	-0.365
100 Ohms	0.026	-0.096	-0.213
200 Ohms	0.000	-0.063	-0.127
400 Ohms	-0.013	-0.047	-0.080
1000 Ohms	-0.022	-0.036	-0.052

Table A.3: Phase Error (in Degrees) Versus Capacitance and Inductance

Capacitance Error (%)	Inductance Error (%)		
	0%	1%	5%
0%	0.000	-0.066	-0.331
-1%	-0.066	-0.132	-0.397
-5%	-0.330	-0.396	-0.661